

ENHANCEMENT OF MECHANICAL Q FOR LOW PHASE NOISE OPTOMECHANICAL OSCILLATORS

Tristan O. Rocheleau, Alejandro J. Grine, Karen E. Grutter, Robert A. Schneider, Niels Quack, Ming C. Wu, and Clark T.-C. Nguyen
University of California, Berkeley, USA

ABSTRACT

A self-sustained Radiation-Pressure driven MEMS ring OptoMechanical Oscillator (RP-OMO) attaining an anchor-loss-limited mechanical Q -factor of 10,400 in vacuum has posted a best-to-date phase noise of -102 dBc/Hz at a 1 kHz offset from a 74 MHz carrier, more than 15 dB better than the best previously published mark [1]. While enhanced optical and mechanical Q both serve to lower the optical threshold power required to obtain oscillation, it is the mechanical Q that ends up having the strongest impact on phase noise [2], much as in a traditional MEMS-based oscillator [3]. This motivates a focus on increased mechanical Q —a challenge in previous such devices measured in air—and requires measurement in the absence of gas-damping using a custom optical vacuum measurement system. The improved phase noise performance of these RP-OMOs is now on par with many conventional MEMS-based oscillators and is sufficient for the targeted chip-scale atomic clock application.

INTRODUCTION

Chip-Scale Atomic Clocks (CSACs) have recently entered the commercial market, offering in volumes less than 10 cc unprecedented long-term stability, with Allan deviations better than 10^{-11} at one hour [4]. MEMS technology is largely responsible for not only the small size of these atomic clocks, but also their ability to operate with substantially lower power consumption (~ 150 mW) than their conventional non-MEMS brethren. In particular, it is a MEMS-based micro-oven that keeps alkali metal atoms in a vapor state while consuming only 5-10 mW of power, all due to a MEMS-enabled enormous thermal resistance.

Despite this already low power consumption versus conventional counterparts, there is still much room for improvement. In a typical CSAC, the micro-oven requires ~ 10 mW, and the control electronics another 10 mW [5]. Interestingly, it is the last major component—the microwave oscillator—that consumes much of the rest, ~ 100 mW. Indeed, it is a very conventional quartz-crystal-based synthesizer, with its power hungry frequency divider, that inevitably limits CSAC power consumption. Here, although replacement of the quartz oscillator by a MEMS-based oscillator offers further size reduction, it does not solve the power problem, since inevitably an output frequency near 10MHz is desired, so some form of power-hungry frequency division would still be required.

This work investigates an approach that could potentially break the power consumption barrier by dispensing with the conventional microwave synthesizer and instead replacing it with a Radiation-Pressure driven OptoMechanical Oscillator (RP-OMO), *cf.* Fig. 1, ideally suited for applications requiring modulated optical outputs, such as CSAC, while still attaining phase noise marks commensurate with a MEMS-based oscillator without the need for frequency division. An RP-OMO consists of a ring or disk-shaped device that acts simultaneously as an optical and a mechanical resonator, which when pumped with

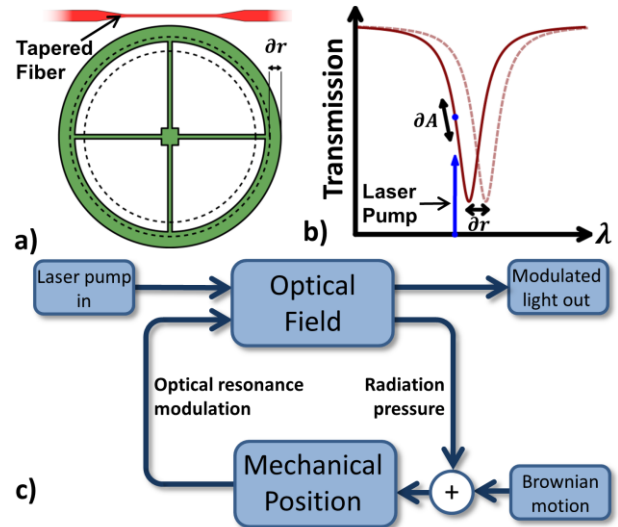


Fig. 1: Operation of an RP-OMO. As the ring resonator coupled to tapered fiber in (a) displaces by δr , the optical path length change produces the shift of the resonance wavelength shown in (b) and subsequently, the circulating power amplitude (and phase), ∂A . With a blue-detuned laser pump, the closed-loop feedback system of (c) is created, where the interaction of optical field and mechanical position produces laser power-dependent parametric amplification of resonator motion.

laser light can be driven into oscillation due to radiation pressure alone. In a typical device, the optical resonance is a whispering gallery mode, capable of high optical Q -factors (Q_0) exceeding 10^8 [6], while the desired mechanical resonance is the radial breathing mode of the ring.

When driven to oscillation, the motion of the RP-OMO ring produces modulated laser light output at the mechanical resonance frequency and, via non-linear mechanical and optical interaction, many higher-order harmonics as well. This efficient harmonic generation opens the potential to generate modulation at 3.4 GHz, the frequency necessary to excite the hyperfine transition in a Rb CSAC application, while operating at a much lower fundamental frequency. Locking the 3.4 GHz harmonic to the Rb transition, as in Fig. 2, transfers the excellent long-term stability of the atomic reference to the RP-OMO, while allowing it to retain its own (superior) short-term stability, governed by its phase noise at its much lower mechanical resonance frequency. This phase noise must satisfy the ultimate application in question, e.g., communications.

Although the first demonstration of an RP-OMO occurred using an ultra-high Q_0 silica resonator [7], the phase noise in such oscillators has typically been poor [8]—a major impediment to real-world applications including the targeted CSAC one. More recently, [1] demonstrated the potential of such devices to be immune to flicker noise, which yielded some improvement, but the performance achieved was still limited by low mechanical Q (Q_m) to -85 dBc/Hz at 1 kHz offset from a 42 MHz carrier.

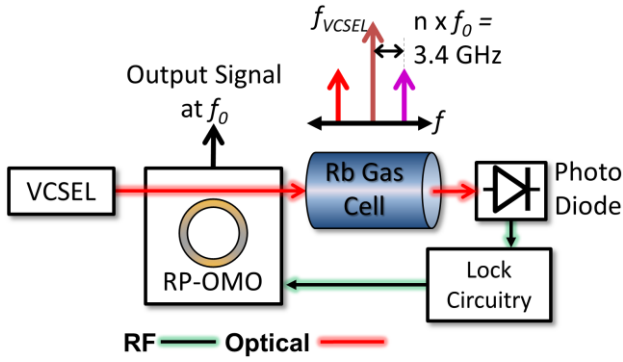


Fig. 2: Target CSAC application using an RP-OMO operating at f_0 , while locking to a Rb gas cell with a 3.4 GHz harmonic.

Here, while both Q_o and Q_m affect the optical threshold power required to obtain oscillation, it is the Q_m that has the largest impact on phase noise [2], much as in a traditional MEMS-based oscillator [3]. This motivates a focus on increased Q_m , which has been a challenge in previous such devices measured in air. The results reported here are enabled by measurement in a custom-made vacuum system that allows exploration of the high Q_m in ring-shaped resonators in the absence of gas damping.

THE RADIATION-PRESSURE DRIVEN OPTOMECHANIC OSCILLATOR

In the RP-OMO as depicted in Fig. 1, blue-detuned (i.e., with shorter wavelength than that of the optical resonance) laser light couples into the optomechanical resonator, producing a Q_o -enhanced radiation pressure force on the outside of the ring. The radiation force displaces the mechanical resonance, increasing the optical path length, and thus intrinsically coupling optical and mechanical modes. In a process analogous to Raman scattering, photons are scattered up in wavelength by the mechanical resonance, producing a parametric amplification of the initially Brownian mechanical motion, which for sufficient optical power, generates a self-sustained oscillation of the mechanical mode. Depicted graphically in Fig. 1c, this interaction is described by the differential equations [9]:

$$\ddot{r}(t) + \Gamma_m \dot{r}(t) + \left(\frac{f_0}{2\pi}\right)^2 = \frac{F_{rp}}{m_{\text{eff}}} \quad (1)$$

$$\begin{aligned} \dot{A}(t) + A(t) \left[\gamma_{\text{tot}} - i\Delta\omega + i\frac{\omega_0}{\tau_o} r(t) \right] \\ = iB \sqrt{\frac{2\pi r_o}{c}} \gamma_{\text{ext}} \end{aligned} \quad (2)$$

where $r(t)$ is the radial displacement of the mechanical resonator from equilibrium, Γ_m is mechanical damping, $\omega_m = 2\pi f_0$ is mechanical resonance frequency, $A(t)$ the optical field in the resonator, $\Delta\omega$ the detuning of laser from optical resonance frequency ω_o , B input pump laser field, γ_{tot} the total optical resonator damping, γ_{ext} the coupling between optical resonator and the tapered fiber, and m_{eff} a mode-dependent mechanical effective mass defined such that $m_{\text{eff}} = 2U/(r_{\text{max}}^2 \omega_m^2)$ with U being total energy stored in the mechanical mode. F_{rp} is the radiation pressure force produced by the circulating light, given by $F_{rp} = 2\pi n P_c / c$, where n is effective index of refraction, c is speed of light, and P_c is the power circulating the cavity.

When driven by a laser, the RP-OMO operates as in Fig. 1, where motion of the ring shifts the optical resonance, modulating the circulating light, which in turn produces feedback in the form of radiation pressure on the mechanical mode. This interplay is similar to traditional oscillator loops with the optical field acting as a parametric amplification on mechanical motion, with the phase of the driving force dependent on the relative detuning of laser to optical resonance and the gain on the optical power. To start-up oscillation, the loop phase-shift of the feedback force must be zero. In addition, the optical power provided by the blue-detuned laser pump must be sufficient to overcome losses towards a positive loop gain.

The RP-OMO is a unique oscillator in that, in principle, the optical feedback may be shot-noise limited; however background thermal noise still exists in the form of Brownian forces on the mechanical resonator. This noise is shaped by the parametric gain and gives rise to phase noise in the final output oscillator spectrum [10]. While the mechanics of amplification and oscillation in the RP-OMO are novel, as with any oscillator the phase noise may be understood in the context of regenerative amplification of thermal noise, shaped by the tank-circuit feedback element [11]. Such a treatment gives rise to the well-known Leeson's equation for phase noise [12]:

$$\mathcal{L}(f) \cong 10 \log \left[\frac{2FkT}{P_{\text{sig}}} \left(1 + \frac{1}{Q^2} \left(\frac{f_0}{2\Delta f} \right)^2 \right) \right] \quad (3)$$

where $\mathcal{L}(f)$ is the single side-band phase noise at an offset Δf from carrier of an oscillator operating with output power P_{sig} and a tank-circuit element with quality factor Q : in this case the mechanical quality factor. Noise factor F expresses the total additive noise in the system and is a function of intrinsic Brownian noise and any additive laser noise. Compared with traditional electronic oscillators, P_{sig} is complicated to measure, but may be calculated as a numerical solution to the coupled differential equations as in [10]. While improvements may be made to P_{sig} , the strong Q_m^2 dependence motivates a primary focus on improving Q_m for decreased phase noise.

Harmonic Generation for Chip-Scale Atomic Clocks

As previously introduced, Fig. 2 presents the future application of a fully-integrated CSAC oscillator system. In this application, a chip-scale Vertical-Cavity Surface-Emitting Laser (VCSEL) provides an output serving as both the optical pump for a RP-OMO and an interrogating laser for the hyper-fine Rubidium transition in an atomic vapor cell.

Once self-sufficient oscillation of the RP-OMO is achieved, the onset of non-linear interaction of optical resonance and mechanical position limits the oscillation amplitude. Interestingly, this nonlinear interaction creates a highly efficient frequency multiplication effect. For the CSAC application, this provides a unique opportunity whereby one of these higher-order harmonics at 3.4 GHz can be used to lock to a Rb gas cell using coherent population trapping [13]. Using the transmitted optical power measurement as feedback to a next-generation version of the RP-OMO with added tuning electrodes enables an amazingly simple and low-power device that simultaneously outputs the high frequency modulation needed for atomic locking, as well as the low 10's of MHz signal desired as an electrical output of a CSAC, without the need for power-hungry frequency division.

Table 1: Theoretical predictions and measured values for the fabricated ring optomechanical resonator devices.

	Design		Measured	
	PSG	Nitride	PSG	Nitride
r_i	45 μm	17 μm	f_0	18.6 MHz / 74.0 MHz
r_o	52.5 μm	25 μm	Q_m (air)	1,050 / 1,800
h	2 μm	370 nm	Q_m (vacuum)	7,200 / 10,400
f_0	19.1 MHz	75.1 MHz	Q_o	2.8×10^6 / 74,000
m_{eff}	11.8 ng	1.2 ng		

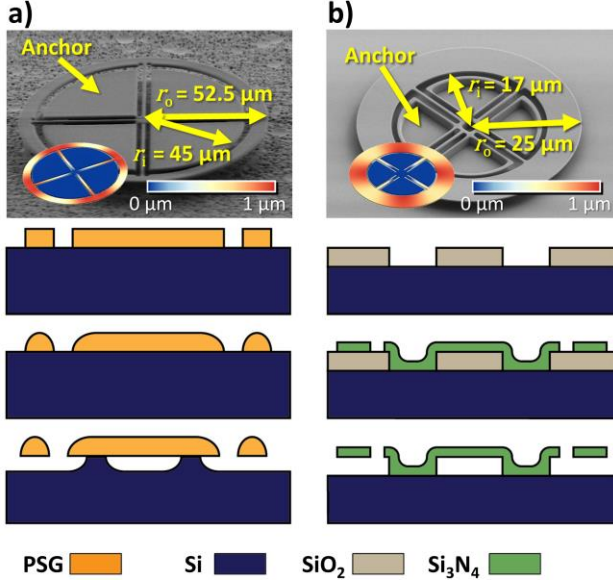


Fig. 3: SEM images and the corresponding fabrication process for (a) PSG devices consisting of LPCVD deposition of PSG, etch in C_4F_8 , reflow at 1050°C , and timed release in XeF_2 ; and (b) nitride devices with an added anchor etch. Nitride is etched with SF_6 , and released in 10:1 BHF. Inset FEM simulations show mode shapes for the fundamental contour mode excited by the optical interaction.

DEVICE DESIGN AND OPERATION

Pursuant to the goal of simultaneous high mechanical and optical Q , the spoke-supported ring design of [14] was used to design the devices of Fig. 3. Such resonators have radially symmetric modes with frequencies defined by the transcendental equations [15]:

$$\begin{aligned} & [J_1(pr_i)\sigma - J_1(pr_i) + r_i p J_0(pr_i)] \\ & \times [Y_1(pr_o)\sigma - Y_1(pr_o) + r_o p Y_0(pr_o)] \\ & - [Y_1(pr_i)\sigma - Y_1(pr_i) + r_i p Y_0(pr_i)] \\ & \times [J_1(pr_o)\sigma - J_1(pr_o) + r_o p J_0(pr_o)] = 0 \end{aligned} \quad (4)$$

$$f_0 = \frac{p}{2\pi} \sqrt{\frac{E}{\rho(1-\sigma^2)}} \quad (5)$$

where r_i is inner ring radius, r_o outer ring radius, ρ material density, σ Poisson's ratio, E Young's modulus, J 's Bessel functions of the first kind, and Y 's Bessel functions of the second kind. While there are an infinite number of solutions to Eq. (4) and (5), corresponding to higher-order modes increasing in frequency, the fundamental mode (FEM simulations of which are seen in the insets of Fig. 3) couples most strongly to the optical resonator and as such is the mode excited into oscillation by the optical force. Table 1 presents the design and measured values for PSG and nitride devices, indicating close agreement.

Fig. 3 presents SEMs and fabrication processes of ring-shaped RP-OMOs made in two materials: phospho-silicate glass (PSG) with modest Q_m and high Q_o ; and stoichiometric silicon-nitride with low Q_o but high Q_m . Fabrication for these devices comprise one or two-mask wafer-scale processes with an added reflow step for PSG devices [16] that enable Q_o 's of 6.5million—a marked improvement over previous state-of-the-art one-by-one laser-annealed devices [7]. Without a smoothing process, nitride devices are limited to $Q_o \sim 100,000$.

Vacuum-Enabled Measurement Setup

Optical interrogation of fabricated devices in vacuum required the construction of the custom vacuum probe system shown in Fig. 4, which provides both optical and electrical interrogation and measurement. Here, light couples in and out of the on-chip RP-OMO via a tapered fiber [17] mounted on a specially-designed three-axis nanopositioning stage. With 10 nm repeatable precision, this system allows accurate coupling and interrogation of RP-OMO devices.

EXPERIMENTAL RESULTS

Fig. 5 presents measurements made on a nitride RP-OMO, exhibiting the typical Lorentzian curves of the optical (Fig. 5a) and mechanical (Fig. 5b) resonances from which Q_o and Q_m are extracted. Fig. 5c provides a first demonstration of the harmonic comb effect desired for the CSAC applications, producing sizable oscillation peaks to

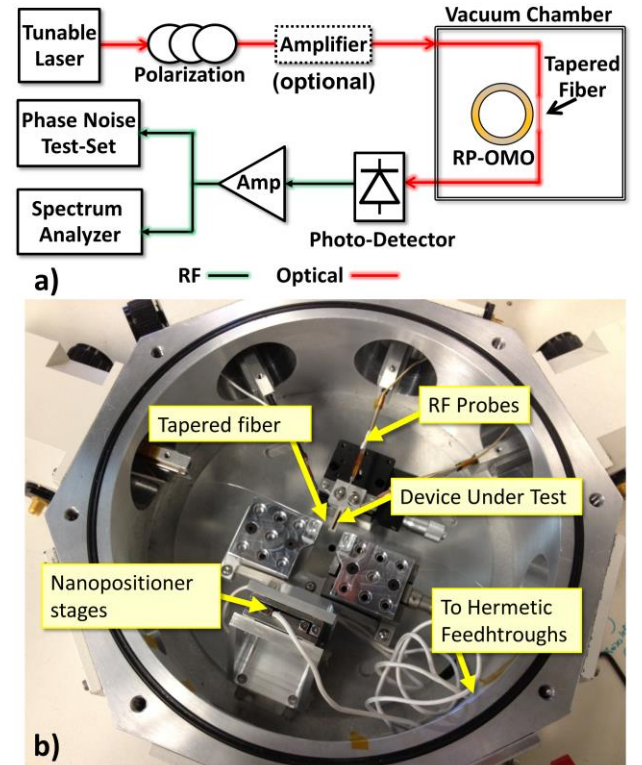


Fig. 4: Experimental measurement setup consisting of (a) the measurement circuit comprised of a Newfocus TLB-6728 tunable laser, optional Erbium-doped fiber amplifier and photo-diode amplifier chain feeding an Agilent N9030A spectrum analyzer and a E5505A phase noise test system; and (b) the custom-built vacuum chamber including tapered-fiber, RF probes and Attocube ECS3040/NUM positioner stages with 10 nm precision.

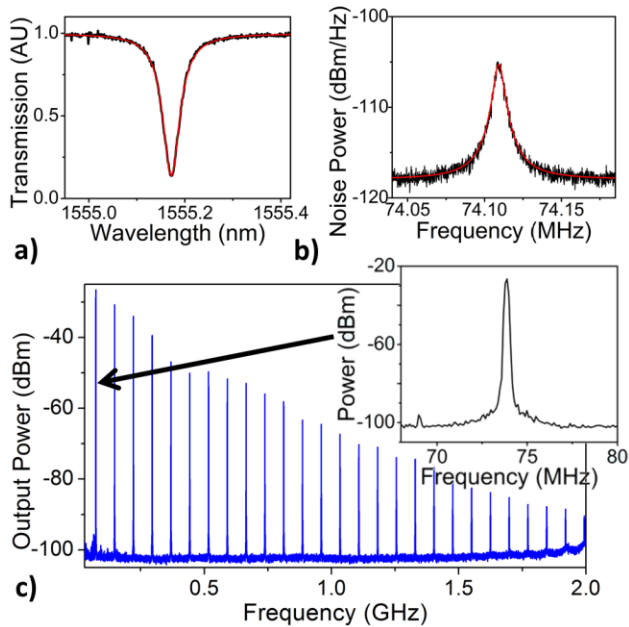


Fig. 5: Measurements of an RP-OMO showing a) an over-coupled optical resonance, b) Brownian motion of a nitride ring measured with low optical power to obtain $Q_m=10,400$, and c) a typical frequency comb produced by an oscillating RP-OMO.

above 2 GHz.

Fig. 6a presents measured phase noise data for the 18.6-MHz PSG RP-OMO, where the phase noise in vacuum is seen to be an impressive 7-9 dB better than in air, achieving -87 dBc/Hz at a 1 kHz offset—better performance than any similar silica-based device posted to date. Besting even this, Fig. 6b shows similar curves for a 74-MHz nitride RP-OMO, yielding a similar 8 dB improvement in vacuum and posting a remarkable -102 dBc/Hz at 1 kHz offset. This improvement in phase noise closely follows that predicted by Eq. (3) for the measured Q_m -enhancement in vacuum.

CONCLUSIONS

Through careful design and measurement in vacuum, fully optomechanical oscillators have been shown to achieve anchor-loss limited Q_m and resulting improvements in phase noise. The performance of these devices has bested all previous phase noise measurements by more than 15 dB, for the first time proving RP-OMO technology as not only suitable for the target CSAC application, but also a viable competitor to previous on-chip MEMS oscillators [3].

Acknowledgement: This work was supported under the DARPA ORCHID program.

REFERENCES:

- [1] S. Tallur, S. Sridaran, and S. Bhawe, *Proceedings, IEEE Int. Conf. on MEMS*, 2012, pp. 19-22.
- [2] A. Grine, N. Quack, K. Grutter, T. Rocheleau, *et al.*, *Proceedings, IEEE Int. Conf. on Opt. MEMS and Nanophotonics*, 2012, pp. 51-52.
- [3] Y. W. Lin, S. Lee, S. S. Li, Y. Xie, *et al.*, *IEEE J. of Solid-State Circuits*, vol. 39, pp. 2477-2491, 2004.
- [4] Symmetricom Product Number SA.45s Specifications
- [5] C. T. C. Nguyen, *IEEE Trans. on Ultrason. Ferroelec. and Freq. Control*, vol. 54, pp. 251-270, 2007.

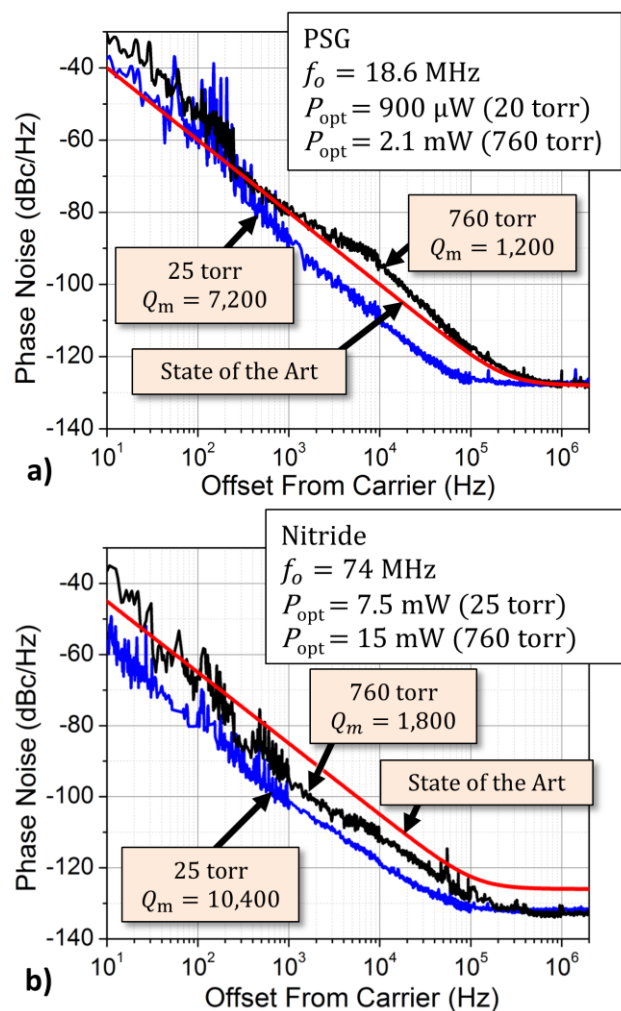


Fig. 6: Measured phase noise of (a) the 18.6-MHz PSG and (b) the 74-MHz silicon-nitride optomechanical oscillators in air (black) and vacuum (blue). For both devices, measurement in a vacuum environment removes air-damping losses, enhancing Q_m closer to device limits. The red curves represent best-to-date published phase noise data for silica [2] and nitride [1] RP-OMOs, scaled by carrier frequency.

- [6] D. Armani, T. Kippenberg, S. Spillane, and K. Vahala, *Nature*, vol. 421, pp. 925-928, 2003.
- [7] H. Rokhsari, T. Kippenberg, T. Carmon, and K. J. Vahala, *Optics Express*, vol. 13, pp. 5293-5301, 2005.
- [8] H. Rokhsari, M. Hossein-Zadeh, A. Hajimiri, and K. Vahala, *App. Phys. Lett.*, vol. 89, pp. 261109-261109-3, 2006.
- [9] H. Rokhsari, T. Kippenberg, T. Carmon, and K. Vahala, *IEEE J. of Selected Topics in Quantum Electronics*, vol. 12, pp. 96-107, 2006.
- [10] M. Hossein-Zadeh, H. Rokhsari, A. Hajimiri, and K. J. Vahala, *Phys. Rev. A*, vol. 74, p. 023813, 2006.
- [11] W. A. Edson, *Proc. of the IRE*, vol. 48, pp. 1454-1466, 1960.
- [12] D. B. Leeson, *Proceedings of the IEEE*, vol. 54, pp. 329-330, 1966.
- [13] N. Cyr, M. Tetu, and M. Breton, *IEEE Trans. on Instr. and Measurement*, vol. 42, pp. 640-649, 1993.
- [14] S. S. Li, Y. W. Lin, Y. Xie, Z. Ren, *et al.*, *Proceedings, IEEE Int. Conf. on MEMS*, 2004, pp. 821-824.
- [15] C. Stephenson, *J. Acoustical Soc. of Am.*, vol. 28, pp. 51-56, 1956.
- [16] K. E. Grutter, A. Grine, M. K. Kim, N. Quack, *et al.*, *Proceedings, CLEO: Sci. and Innov.*, 2012.
- [17] J. Knight, G. Cheung, F. Jacques, and T. Birks, *Optics letters*, vol. 22, pp. 1129-1131, 1997.